Internet Appendix

Vaccine Progress, Stock Prices, and the Value of Ending the Pandemic

August 2023

Appendix A contains proofs of the propositions in Section 2 of the paper, and discusses further the output claim and alternative representations of the market portfolio.

Appendix B includes additional details on construction of the vaccine progress indicator as described in Section 3.

Appendix C presents extensions of the model to include (i) endogenous investment in a mitigation technology, (ii) endogenous pandemic severity via labor choice, and (iii) agents who do not participate in the stock market.

Appendix D discusses the experiences of the stock market and consumption during 2020 as interpreted through the lens of the model.

A Proofs

A.1 Proof of Proposition 1

Proposition 1. *Denote*

$$g(s) \equiv \frac{(1-\gamma)\rho}{(1-\psi^{-1})} - (1-\gamma)\left(\mu(s) - \frac{1}{2}\gamma\sigma(s)^2\right) - \zeta(s)\left([1-\chi(s)]^{1-\gamma} - 1\right) \tag{A.1}$$

Assume all state parameters are constant for $0 < s < S$. Let $H(s)$'s denote the solution to the following system of S recursive equations:

$$g_0 \equiv g(0) = \frac{(1-\gamma)}{(\psi-1)}\rho^{\psi}\left(H(0)\right)^{-\psi\theta^{-1}} + \eta\left[\frac{H(1)}{H(0)} - 1\right] \tag{A.2}$$

$$g_1 \equiv g(1) = \frac{(1-\gamma)}{(\psi-1)}\rho^{\psi}\left(H(s)\right)^{-\psi\theta^{-1}} + \lambda_d\left[\frac{H(s-1)}{H(s)} - 1\right] + \lambda_u\left[\frac{H(s+1)}{H(s)} - 1\right], \tag{A.3}$$

for $s \in \{1,\ldots,S-1\}$.

Assuming the solutions are positive, optimal consumption in state s is

$$C(s,q) = \rho^{\psi}\ \left(H(s)\right)^{-\psi\theta^{-1}}\ q, \tag{A.4}$$

and the value function of the representative agent is

$$\mathbb{J}(s,q) \equiv \frac{H(s)q^{1-\gamma}}{1-\gamma}. \tag{A.5}$$

Proof. From the evolution of capital stock for the representative agent (8), we obtain the Hamilton-Jacobi-Bellman (HJB) equation as follows for each state s:

$$\begin{aligned} 0 = \max_{C}\Big[& f(C,\mathbb{J}) - \rho\mathbb{J}(s,q) + \mathbb{J}_q(s,q)(q\mu(s) - C) \\ & + \frac{1}{2}\mathbb{J}_{qq}(s,q)q^2\sigma(s)^2 + \zeta(s)\left[\mathbb{J}(s,q(1-\chi(s)) - \mathbb{J}(s,q)\right] \\ & + \lambda_u(s)\left[\mathbb{J}(s+1,q) - \mathbb{J}(s,q)\right] + \lambda_d(s)\left[\mathbb{J}(s-1,q) - \mathbb{J}(s,q)\right]\Big] \end{aligned} \tag{A.6}$$

where for $s = 0, s = S$ we interpret $\chi(s) = 0, \zeta(s) = 0$ and $\lambda_u(s) = \eta, \lambda_d(s) = 0$.

Taking the first-order condition with respect to $C(s,q)$ in HJB equation (A.6), we obtain

$$f_c(C,\mathbb{J}(s,q)) - \mathbb{J}_q(s,q) = 0. \tag{A.7}$$

Using $f(C,\mathbb{J})$ from (10) and taking the derivative with respect to C, we obtain

$$f_c = \frac{\rho C^{-\psi^{-1}}}{[(1-\gamma)\mathbb{J}]^{\frac{1}{\theta}-1}}. \tag{A.8}$$

Substituting the conjecture $\mathbb{J}(s,q)$ in equation (A.5) yields

$$f_c = \frac{\rho C^{-\psi^{-1}}}{H(s)^{\frac{\gamma-\psi^{-1}}{1-\gamma}} q^{\gamma-\psi^{-1}}}. \tag{A.9}$$

Then, for state $s \in \{0,\ldots,S\}$, we obtain by substituting $\mathbb{J}_q(s,q) = H(s)q^{-\gamma}$ in (A.7), and simplifying:

$$C(s,q) = \frac{H(s)^{-\theta\psi^{-1}} q}{\rho^{-\psi}}. \tag{A.10}$$

To verify the conjectured form of the value function, we plug it in to the HJB equation (A.6) and reduce it to the recursive system in the proposition via the following steps:

1. substitute the optimal policy $C(s)$ into the HJB equation (A.6);
2. cancel the terms in q which have the same exponent; and
3. group terms not involving $H(s)$ into $g(0)$ for state $s = 0$ and $g(s)$ for state $s \in \{1,\ldots,S-1\}$

to reach equations (A.1) – (A.3). This system of recursive equations can be solved numerically with the final condition $H(S) = H(0)$, that states 0 and S are non-disaster states.

□

A.2 Proof of Proposition 2

Proposition 2. *The welfare gain to ending the disaster state s is determined by the ratio of marginal propensity to consume ($c \equiv dC/dq$) in the disaster state s relative to that in the non-disaster state, adjusted by the agent's elasticity of intertemporal substitution (EIS):*

$$V(s) = 1 - \left(\frac{c(s)}{c(0)}\right)^{-\frac{1}{\psi-1}} = 1 - \left(\frac{C(s)}{C(0)}\right)^{-\frac{1}{\psi-1}} \tag{A.11}$$

Proof. The proposition just follows from substituting for $C(s,q)$ from (A.4) into the definition of $V(s)$. □

A.3 Proof of Proposition 3

Proposition 3. *The price of the output claim is $P = p(s)q$ where the constants $p(s)$ solve a matrix system $Y = Xp$ where X is an $S+1$-by-$S+1$ matrix and Y is an $S+1$ vector both of whose elements are given in the appendix.*

Proof. To begin, we derive the pricing kernel and the risk-free rate. Under stochastic differential utility, the kernel can be represented as

$$\Lambda_t = e^{\int_0^t f_{\mathbb{J}} du} f_C \tag{A.12}$$

where

$$f(C,J) = \rho \frac{C^{\varrho}}{\varrho} \left((1-\gamma)\mathbb{J}\right)^{1-\frac{1}{\theta}} - \rho\theta\mathbb{J} \tag{A.13}$$

where $\varrho = 1 - \frac{1}{\psi}, \theta = \frac{1-\gamma}{\varrho}$. As established above, the value function and the consumption flow rates are:

$$\mathbb{J} = q^{1-\gamma} H(s)/(1-\gamma) \quad \text{and} \quad C = \rho^{\psi} H(s)^{e}\, q \tag{A.14}$$

where $e = \frac{1-\psi}{1-\gamma}$. Together these imply

$$f_C = \rho C^{\varrho-1} \left((1-\gamma)\mathbb{J}\right)^{1-\frac{1}{\theta}} \tag{A.15}$$

or

$$f_C = \rho \left(\rho^{\psi} H(s)^e q\right)^{\varrho-1} \left((1-\gamma)\left(q^{1-\gamma} H(s)/(1-\gamma)\right)\right)^{1-\frac{1}{\theta}}. \tag{A.16}$$

Simplifying, we get:

$$f_C = \rho^{1+\psi(\varrho-1)} H(s)^{e(\varrho-1)+\frac{\theta-1}{\theta}} q^{(\varrho-1)+\frac{(1-\gamma)(\theta-1)}{\theta}}. \tag{A.17}$$

The exponent of ρ is: $1+\psi(\varrho-1) = 1+\psi(-\frac{1}{\psi}) = 0$. The exponent of q is: $(\varrho-1) + \frac{(1-\gamma)(\theta-1)}{\theta}$. Substitute $\theta = \frac{1-\gamma}{\varrho}$ to get: $(\varrho-1)+\varrho(\frac{1-\gamma}{\varrho}-1) = -\gamma$. The exponent of $H(s)$ is

$$e(\varrho-1) + \frac{\theta-1}{\theta} \Rightarrow \frac{1-\psi}{1-\gamma}\left(-\frac{1}{\psi}\right) + \frac{1-\gamma\psi}{\psi(1-\gamma)} = 1 \tag{A.18}$$

Hence, $f_C = H(s)q^{-\gamma}$. Next, to evaluate $f_{\mathbb{J}}$, note that

$$f_{\mathbb{J}} = \rho \frac{C^{\varrho}}{\varrho}\left(1-\frac{1}{\theta}\right)\left[(1-\gamma)\mathbb{J}\right]^{-\frac{1}{\theta}}(1-\gamma) - \rho\theta \tag{A.19}$$

Plugging in for C and $\mathbb{J}$ we get:

$$f_{\mathbb{J}} = \rho \frac{\left(\rho^{\psi} H(s)^e q\right)^{\varrho}}{\varrho}\left(1-\frac{1}{\theta}\right)\left[(1-\gamma)\left(q^{1-\gamma}H(s)/(1-\gamma)\right)\right]^{-\frac{1}{\theta}}(1-\gamma) - \rho\theta \tag{A.20}$$

This can be expressed as

$$f_{\mathbb{J}} = \frac{1}{\varrho}\rho^{1+\psi\varrho} H(s)^{e\varrho-\frac{1}{\theta}} q^{\varrho+\frac{\gamma-1}{\theta}}\left(\frac{\theta-1}{\theta}\right)(1-\gamma) - \rho\theta. \tag{A.21}$$

Here the exponent of ρ is : $1+\psi\varrho = \psi$, and the exponent of $H(s)$ is: $e\varrho - \frac{1}{\theta} = e\varrho - \frac{\varrho}{1-\gamma} = e$, and the exponent of q is: $\varrho + \frac{\gamma-1}{\theta} = 0$. Hence,

$$f_{\mathbb{J}} = \frac{1}{\varrho}\rho^{\psi} H(s)^e \left(\frac{\theta-1}{\theta}\right)(1-\gamma) - \rho\theta = \rho^{\psi} H(s)^e(\theta-1) - \rho\theta = c(s)(\theta-1) - \rho\theta. \tag{A.22}$$

So, we conclude that

$$\Lambda_t = e^{\int_0^t f_{\mathbf{J}} du} f_C = q^{-\gamma} H(s) e^{\int_0^t [c(s)(\theta-1)-\rho\theta] du}. \tag{A.23}$$

The riskless interest rate, $r(s)$ is minus the expected change of $d\Lambda/\Lambda$ per unit time. Applying Itô's lemma to the above expression yields drift (or dt terms)

$$c(s)\ (\theta-1) - \rho\theta - \gamma(\mu(s) - c(s)) + \gamma(\gamma+1)\sigma(s)^2 \tag{A.24}$$

Note that the term $(\mu - c)$ is the drift of dq/q. To these terms we add the expected change from the jumps in the state s for $s = 0$:

$$\eta\ \left(\frac{H(1)}{H(0)} - 1\right) \equiv \tilde{\eta} - \eta \tag{A.25}$$

which serves to define the risk-neutral jump intenstity $\tilde{\eta}$. For $s > 0$ the expected jumps include both up and down changes in s as well as jumps in $q^{-\gamma}$:

$$\lambda_u\ \left(\frac{H(s+1)}{H(s)} - 1\right) + \lambda_d\ \left(\frac{H(s-1)}{H(s)} - 1\right) + \zeta((1-\chi)^{-\gamma} - 1) \equiv (\tilde{\lambda_u} - \lambda_u) + (\tilde{\lambda_d} - \lambda_d) + (\tilde{\zeta} - \zeta) \tag{A.26}$$

where the risk neutral intensities $\tilde{\lambda_u}, \tilde{\lambda_d}$ are defined as for η.[1]

The full expression for $r(0)$ is then

$$-\left\{c(0)\ (\theta-1) - \rho\theta - \gamma(\mu - c(0)) + \gamma(\gamma+1)\sigma^2 + (\tilde{\eta} - \eta)\right\}. \tag{A.27}$$

For $s > 0$ we have $r(s)$ as

$$-\left\{c(s)(\theta-1) - \rho\theta - \gamma(\mu(s) - c(s)) + \frac{1}{2}\gamma(\gamma+1)\sigma(s)^2 + (\tilde{\lambda_u} - \lambda_u) + (\tilde{\lambda_d} - \lambda_d) + (\tilde{\zeta} - \zeta))\right\}. \tag{A.28}$$

[1]The notation suppresses the dependence of these quantities on the state s.

A helpful simplification is to observe that, by the HJB equations derived above, the $(\tilde{\eta} - \eta)$ terms in the first expression can be replaced by $g_0 - \frac{\theta}{\psi}c(0)$. This causes all of the terms involving $c(0)$ to exactly cancel. Using the definition of g_0 in (A.1), the remaining terms also simplify, and we arrive at.

$$r(0) = \mu(0) - \gamma\sigma(0)^2.$$

The same replacement works analogously for the second expression and yields

$$r(1) = \mu(1) - \gamma\sigma(1)^2 - \zeta\chi(1-\chi)^{-\gamma}.$$

We return to these expressions below.

By the fundamental theorem of asset pricing, the instantaneous expected excess return to the claim $P(q,s)$ must equal minus covariance of the returns to P with the pricing kernel. Deriving these two quantities and setting them equal yields the pricing system, to which the proof will construct the solution.

The expected excess return to the claim $P(q,s)$ is the sum of its expected capital gain and its expected payout, minus rP. In the nondisaster state, this is

$$\frac{1}{2}\sigma(0)^2q^2P_{qq}(q,0) + (\mu(0) - c(0))qP_q(q,0) + \eta(P(q,1) - P(q,0)) + \mu(0)q - r(0)P(q,0) \tag{A.29}$$

whereas in the disaster states it is

$$\begin{aligned}&\frac{1}{2}\sigma(s)^2q^2P_{qq}(q,s) + (\mu(s) - c(s))qP_q(q,s)\\ &+\lambda_u(P(q,s+1) - P(q,s)) + \lambda_d(P(q,s-1) - P(q,s)) + \zeta(P((1-\chi)q,s) - P(q,s))\\ &+\mu(s)q - \zeta\chi q - r(s)P(q,s).\end{aligned} \tag{A.30}$$

Next, we need to derive the covariance of the returns to P with $d\Lambda/\Lambda$. In addition to

the usual contribution of covariance from the capital gains dP/P, the covariance also includes the contribution from the dividends themselves, which are risky in this model. There are also contributions from both Brownian comovement and co-jumps in q and s. The Brownian terms are

$$-\gamma\sigma(s)^2[qP_q(q,s)+q]. \tag{A.31}$$

The co-jump terms for $s>0$ are

$$\begin{aligned}&\zeta[P((1-\chi)q,s)-P(q,s)-\chi q]\left[(1-\chi)^{-\gamma}-1\right]\\&+\lambda_u[P(q,s+1)-P(q,s)]\left[\frac{H(s+1)}{H(s)}-1\right]+\lambda_d[P(q,s-1)-P(q,s)]\left[\frac{H(s-1)}{H(s)}-1\right]\end{aligned} \tag{A.32}$$

or

$$\begin{aligned}&[P((1-\chi)q,s)-P(q,s)-\chi q]\left[\tilde{\zeta}-\zeta\right]\\&+[P(q,s+1)-P(q,s)][\tilde{\lambda_u}-\lambda_u]+[P(q,s-1)-P(q,s)][\tilde{\lambda_d}-\lambda_d].\end{aligned} \tag{A.33}$$

For $s=0$ the corresponding expression is just

$$[P(q,1)-P(q,0)][\tilde{\eta}-\eta]. \tag{A.34}$$

We now equate the expected excess return to minus the above covariance to obtain the difference/differential equation system that P must solve. Rather than repeating the general expressions, we conjecture that the solutions are linear in q and deduce the resulting system. Under linearity $P_{qq}=0$ and $P_q=p$, a constant that depends on s.

Plugging in the conjectured form, and cancelling a q, in states $s>0$ the pricing equation says

$$(\mu(s)-c(s))p(s)+\lambda_u(p(s+1)-p(s))+\lambda_d(p(s-1)-p(s)) \tag{A.35}$$

$$-\chi\zeta p(s)+\mu(s)-\zeta\chi-r(s)p(s)-\gamma\sigma(s)^2[p(s)+1] \tag{A.36}$$

$$-\chi[p(s)+1]\left[\tilde{\zeta}-\zeta\right]+[p(s+1)-p(s)][\tilde{\lambda_u}-\lambda_u]+[p(s-1)-p(s)][\tilde{\lambda_d}-\lambda_d]$$

$$= 0. \tag{A.37}$$

Leaving the constant terms on the left, the right side consists of

$$p(s+1) \quad \text{terms:} \quad -\lambda_u - [\tilde{\lambda_u} - \lambda_u] = -\tilde{\lambda_u}, \tag{A.38}$$

$$p(s-1) \quad \text{terms:} \quad -\lambda_d - [\tilde{\lambda_d} - \lambda_d] = -\tilde{\lambda_d}, \tag{A.39}$$

and $p(s)$ terms:

$$-(\mu(s) - c(s)) + \lambda_u + \lambda_d + \chi\zeta + r(s) + \gamma\sigma(s)^2 + \chi[\tilde{\zeta} - \zeta] + [\tilde{\lambda_u} - \lambda_u] + [\tilde{\lambda_d} - \lambda_d] \tag{A.40}$$

or

$$r(s) + c(s) - (\mu(s) - \gamma\sigma(s)^2) + \tilde{\lambda_u} + \tilde{\lambda_d} + \chi\tilde{\zeta} = c(s) + \tilde{\lambda_u} + \tilde{\lambda_d} \tag{A.41}$$

where the last equality follows from our expression above for $r(s)$.

The remaining constants on the left are

$$\mu(s) - \zeta\chi - \gamma\sigma(2)^2 - \chi[\tilde{\zeta} - \zeta]. \tag{A.42}$$

or

$$(\mu(s) - \gamma\sigma(s)^2) - \chi\tilde{\zeta} = r(s). \tag{A.43}$$

The above equations define a linear system for $p(1)$ to $p(S-2)$. For $p(S-1)$ we have

$$[c(s) + \tilde{\lambda_u} + \tilde{\lambda_d}]p(S-1) - \tilde{\lambda_d}p(S-2) - \tilde{\lambda_u}p(0) = r(S-1).$$

The pricing equation for $s = 0$ says

$$(\mu - c(s))p(0) + \eta(p(1) - p(0)) + \mu - r(0)p(0) - \gamma\sigma^2[p(0) + 1] + [p(1) - p(0)][\tilde{\eta} - \eta] = 0, \tag{A.44}$$

or

$$\mu - \gamma\sigma^2 = r(0) = p(0)[c(0) + \tilde{\eta}] - p(1)\,\tilde{\eta} \tag{A.45}$$

Altogether the system may be written in matrix form,

$$\begin{bmatrix} c(0)+\tilde{\eta} & -\tilde{\eta} & 0 & \cdots \\ -\tilde{\lambda_d} & c(1)+\tilde{\lambda_d}+\tilde{\lambda_u} & -\tilde{\lambda_u} & 0 \\ 0 & \ddots & \ddots & \ddots \\ \vdots & \ddots & \ddots & \ddots \\ -\tilde{\lambda_u} & 0 & \cdots & \end{bmatrix} p = \begin{bmatrix} r(0) \\ r(1) \\ \vdots \\ \vdots \\ \vdots \end{bmatrix}.$$

Assuming consumption is positive, the right-hand matrix is of full rank. Hence the system has a unique, finite solution.

□

A.4 Proof of Proposition 4

Proposition 4. *Given a set of non-disaster parameters (e.g., those given in Table 1) and subject to regularity conditions given in the proof, a particular fixed value of* $A \equiv \frac{\Delta \log P}{\Delta \mathbb{E}[T^\star]}$ *restricts the disaster parameters such that the quantity* $B \equiv \frac{V}{\mathbb{E}[T^\star]}$ *must lie in a finite range* $[\overline{B}, \underline{B}]$*. For large, S, the limits of the range are determined by the solution to a three-equation system given in the proof.*

The proof of the proposition proceeds via a series of lemmas. For ease of notation, the dependence of parameters on the state will be indicated via subscripts, e.g., c_0, c_1, c_s in place of $c(0), c(1), c(s)$.

Lemma A.1. *The HJB system of equations for the value functions* $H(s)$ *depends only on the disaster parameters via the scalar* g_1 *(defined in Proposition 1). Given* g_1*, the linear system of equations for the price of the output claim,* $Xp = Y$*, (given in the proof of Proposition 3) only depends on the disaster parameters via the constant scalar* r_1*, which is elements* 2*...S of the right-hand side vector,* Y*.*

Proof. The statements can be verified directly from the proofs of the respective propositions. Note that the matrix X in the second system definitely does depend on the solution to the first system, and hence on the disaster parameters. But the first statement ensures that that dependence is entirely determined by g_1. Note that Proposition 3 does use the assumption that the disaster parameters do not vary with s during the disaster. □

Lemma A.2. *Assume disasters are worse states in the sense that $\mu_0 \geq \mu_1$ and $\sigma_0 \leq \sigma_1$. Then, for a fixed value of g_1, values of r_1 must lie in a finite range given as the argmin and argmax over the disaster parameters $(\mu_1, \sigma_1, \chi, \zeta)$ subject to the above constraints. Hereafter, assume $\gamma > 1$. The maximization problem has a solution at $\mu_1 = \frac{1}{2}\gamma\sigma_0^2 + (\frac{\rho\theta - g_1}{1-\gamma}), \sigma_1 = \sigma_0, \chi = 0$. The minimization problem has a solution at $\mu_1 = \mu_0, \sigma_1^2 = \frac{2}{\gamma}[\mu_0 - (\frac{\rho\theta - g_1}{1-\gamma})], \chi = 0$. (In both cases ζ is unidentified).*

Proof. Formally, the quantity we are varying is

$$r_1 = \mu_1 - \gamma\sigma_1^2 - \zeta\chi(1-\chi)^{-\gamma}$$

subject to the nonlinear constraint

$$\rho\theta - (1-\gamma)(\mu_1 - \tfrac{1}{2}\gamma\sigma_1^2) - \zeta((1-\chi)^{1-\gamma} - 1) = g_1$$

as well as the bounds on μ_1 and σ_1, and the physical constraints $\zeta \geq 0, 1 > \chi \geq 0$.

First, consider the maximixation problem. We establish (i) starting at $\chi > 0$, the objective can be increased along the constraint for a lower value of χ; then (ii) with $\chi = 0$, the objective can be increased along the constraint by increasing χ and decreasing σ_1 unless its lower bound is binding. Hence, once the σ_1 constraint is hit, the objective can only increase by decreasing χ to zero.

For (i), consider lowering the ζ term in the constraint by an amount $\delta > 0$. The constraint then requires reducing $\mu_1 - \frac{1}{2}\gamma\sigma_1^2$ by $\frac{\delta}{\gamma-1} > 0$. The latter entails a change in the objective of $-\frac{\delta}{\gamma-1} - \frac{1}{2}\gamma\Delta\sigma_1^2$. This (negative) change can be minimized by taking $\Delta\sigma_1^2 = 0$, that is we put $\Delta\mu_1 = -\frac{\delta}{\gamma-1}$ and there is no downside limit on μ_1. Then the overall change in the objective is $-\frac{\delta}{\gamma-1}$ plus the change in its ζ term. If we choose to keep ζ fixed, then the change in the third term is

$$\delta\frac{\Delta(\chi(1-\chi)^{-\gamma})}{\Delta((1-\chi)^{1-\gamma} - 1)}. \tag{A.46}$$

It is straightforward to show that the ratio of first derivatives (a) is equal to $\frac{1}{\gamma-1}$ at $\chi = 0$ and (b) is itself increasing in χ. Hence at any $\chi > 0$ this term exceeds $\frac{\delta}{\gamma-1}$. Hence the objective has increased. This establishes (i).

For (ii), we are now considering increasing χ from zero by an amount such that the ζ

term in the constraint increases by $\delta > 0$. This allows us to increase $\mu_1 - \frac{1}{2}\gamma\sigma_1^2$ by $\frac{\delta}{\gamma-1} > 0$. The latter changes the objective by $\frac{\delta}{\gamma-1} - \frac{1}{2}\gamma\Delta\sigma_1^2$, which we can maximize by taking $\Delta\sigma_1^2 < 0$ unless we are at the constrained lower bound. Meanwhile, the change in the third term (substituting out ζ) is

$$-\delta\frac{\chi(1-\chi)^{-\gamma}}{(1-\chi)^{1-\gamma}-1}. \tag{A.47}$$

By l'Hôpital's rule, the ratio has limit as $\chi \downarrow 0$ of $\frac{1}{\gamma-1}$. Hence this term lowers the objective by less than the increase from the $\mu_1 - \gamma\sigma_1^2$ term, unless we are at the constrained lower bound, in which case the objective cannot be increased.

The claim about the minimization solution is established by analogous steps: (i) in a neighborhood of $\chi = 0$, the objective can be decreased along the constraint by decreasing χ; (ii) with $\chi = 0$, the objective can be decreased along the constraint by increasing χ and increasing μ_1 until its upper bound is binding.

For (i), consider lowering the ζ term in the constraint by an amount $\delta > 0$. The constraint then requires reducing $\mu_1 - \frac{1}{2}\gamma\sigma_1^2$ by $\frac{\delta}{\gamma-1} > 0$. The latter entails a change in the objective of $-\frac{\delta}{\gamma-1} - \frac{1}{2}\gamma\Delta\sigma_1^2$. This change is maximally negative when $\Delta\mu_1 = 0$ and $\frac{1}{2}\gamma\Delta\sigma_1^2 = \frac{\delta}{\gamma-1} > 0$ and there is no upside limit on σ_1. Then the overall change in the objective is $-2\frac{\delta}{\gamma-1}$ plus the change in its ζ term. As above, this term changes by the ratio in (A.46), which is less than $2\frac{\delta}{\gamma-1}$ in a neighborhood of $\chi = 0$.

For (ii), we are now considering increasing χ from zero by an amount such that the ζ term in the constraint increases by $\delta > 0$. This requires us to increase $\mu_1 - \frac{1}{2}\gamma\sigma_1^2$ by $\frac{\delta}{\gamma-1} > 0$. The latter raises the objective by $\frac{\delta}{\gamma-1} - \frac{1}{2}\gamma\Delta\sigma_1^2$. We can thus lower the objective by taking $\Delta\sigma_1^2 > 0$ which we can do as long as μ_1 is not at its upper limit. Meanwhile, the change in the third term is again given by (A.47), which cancels the increase of $\frac{\delta}{\gamma-1}$ insuring that the objective function has increased.

□

Lemma A.3. *Fixing the nondisaster parameters, define* $A(r_1; g_1)$ *as* $\lim_{s\to S}\frac{\Delta \log P}{\Delta \mathbb{E}[T^\star]}$. *Assume* $\lambda_d = 0$. *Then, for large* S,

$$A(r_1) = c_0\left(1 - \frac{r_1(1+\tilde{\eta}/\lambda_0)}{r_0 + r_1\tilde{\eta}/\lambda_1}\right) \tag{A.48}$$

where λ_0, λ_1 are defined in the proof. Assume the parameters satisfy $r_0 > \underline{c}_0 \equiv \frac{\psi-1}{1-\gamma} g_0$. Then A is an increasing function of r_1.

Define $\overline{A}(g_1) = A(r_1^{min}(g_1))$ and $\underline{A}(g_1) = A(r_1^{max}(g_1))$ where r_1^{min}, r_1^{max} are the upper and lower limits found in the previous lemma. For any fixed value $A^\star > 0$, the solutions to

$$\underline{A}(g_1) = A^\star \tag{A.49}$$

$$\overline{A}(g_1) = A^\star \tag{A.50}$$

exist and are finite. Denote these solutions as g_L and g_U respectively.

Proof. The first part of the proof requires explicitly solving for the price vector p via Gaussian elimination. To anticipate one step (and simplify notation), we note that, for large S, the welfare ratio $H(s+1)/H(s)$ between successive steps converges to 1. Hence, the quantity $\tilde{\lambda_{u,s}} = \lambda_u H(s+1)/H(s)$ can be replaced by λ_u. With $\lambda_d = 0$, the system then is[2]

$$\begin{bmatrix} d_0 & -\tilde{\eta} & 0 & \cdots \\ 0 & d_1 & -\lambda_u & 0 \\ 0 & \ddots & \ddots & \ddots \\ \vdots & \ddots & \ddots & \ddots \\ -\lambda_u & 0 & \cdots & d_S \end{bmatrix} p = \begin{bmatrix} r_0 \\ r_1 \\ \vdots \\ \vdots \\ \vdots \end{bmatrix}.$$

where $d_0 = c_0 + \tilde{\eta}, d_s = c_s + \lambda_u$. Interchanging the equations from rows 1 and $S+1$, the algorithm successively eliminates all of the nonzero elements in the bottom row until only the $(S+1, S+1)$ diagonal remains. None of the other rows is affected. Write the solved system as

$$\begin{bmatrix} -\lambda_u & 0 & \cdots & d_S \\ 0 & d_1 & -\lambda_u & 0 \\ 0 & \ddots & \ddots & \ddots \\ \vdots & \ddots & \ddots & \ddots \\ 0 & 0 & \cdots & x \end{bmatrix} p = \begin{bmatrix} r_1 \\ \vdots \\ \vdots \\ \vdots \\ y \end{bmatrix}.$$

We give expressions for x and y below. With them, the system immediately tells us $p_S = y/x$ and $p_{S-1} = \frac{r_1 + \lambda_u p_S}{d_{S-1}}$. The quantity we are trying to compute is then the large-S limit of $\lambda_u(p_S - p_{S-1})/p_S$.

[2] See the proof of Proposition 3.

Straightforward algebra yields the diagonal element x as

$$d_0 \frac{d_S}{\lambda_u} - \tilde{\eta} \prod_{s=1}^{S} \left(\frac{\lambda_u}{d_s} \right)$$

Replacing λ_u by λS, the first term converges to $d_0 = c_0 + \tilde{\eta}$. The product in the second term becomes

$$\prod_{s=1}^{S} \left(\frac{1}{1 + \frac{c_s/\lambda}{S}} \right)$$

which converges to $e^{-\bar{c}/\lambda}$ where $\bar{c} = \lim \frac{1}{S} \sum_s^S c_s$. So we obtain the limit

$$x = c_0 \left(1 + \tilde{\eta}(1 - e^{-\bar{c}/\lambda})/c_0) \right) \equiv c_0 \left(1 + \tilde{\eta}/\lambda_0 \right)$$

where the last expression defines the quantity λ_0.

The successive steps of Gaussian elimination render the right side element y as

$$r_0 + r_1 \left(\frac{d_0}{\lambda_u} + \frac{\tilde{\eta}}{d_1} \left(1 + \sum_{s=1}^{S} \prod_{k=1}^{s} \frac{\lambda_u}{d_{k+1}} \right) \right).$$

The sum in the inner parentheses divided by d_1 converges to $\lim \frac{1}{\lambda S} \sum_{s=1}^{S} e^{\sum_{k=s}^{S} c_k/\lambda S}$, which we will denote $1/\lambda_1$. The term $\frac{d_0}{\lambda_u}$ goes to zero, and we end up with

$$y = r_0 + r_1 \tilde{\eta}/\lambda_1.$$

Returning to $A = \lambda_u (p_S - p_{S-1})/p_S$, replacing λ_u by λS and using $c_S \to c_0$, we find

$$A \to c_0 - r_1 \frac{x}{y} = c_0 \left(1 - \frac{1 + \tilde{\eta}/\lambda_0}{\frac{r_0}{r_1} + \tilde{\eta}/\lambda_1} \right)$$

which is the same as (A.48).

Differentiating the above expression with respect to r_1 establishes that a sufficient condition for A to be decreasing in r_1 is that $r_0 > 0$ which is guaranteed by the assumption $r_0 > \underline{c}_0$.

The next part of the lemma concerns properties of $\overline{A}(g_1)$ and $\underline{A}(g_1)$. We have just seen that $\overline{A} \geq \underline{A}$. Also, if $g_0 = g_1$, the disaster state and the nondisaster state have the same value functions and $r_0 = r_1 = r_1^{min} = r_1^{max}$. This implies that $\overline{A}(g_0) = \underline{A}(g_0) = 0$.

Given these properties, the conclusion of the lemma follows if we can show that $\overline{A}(g_1)$ and $\underline{A}(g_1)$ are continuous and that $\underline{A}(g_1)$ is unbounded as g_1 decreases. These are sufficient to ensure that (A.49) - (A.50) have solutions. The complicating factor in proving these properties is that, as g_1 varies, the solution to the HJB system changes, which means that some quantities (e.g. the consumption propensities c_s) that enter into the function A also vary with g_1 in manners that are not easy to characterize. Our approach is to identify a third function $\underline{C} < \underline{A}$ and show that it is unbounded as g_1 declines.[3]

Now write

$$\underline{A} = c_0 \left(1 - r_1^{max} \frac{1 + \tilde{\eta}/\lambda_0}{r_0 + r_1^{max}\tilde{\eta}/\lambda_1}\right)$$

We are considering the behavior as g_1 declines (worse disasters) and r_1^{max} is also declining. So assume g_1 is sufficiently negative to insure $r_1^{max} < 0$. In that case, making the $\tilde{\eta}$ term in the numerator smaller (less positive) lowers the right side. Likewise, as long as prices remain positive, the denominator is positive. Hence, making the $\tilde{\eta}$ term in the denominator smaller (less negative) also lowers the right side. We can conclude that

$$\underline{A} > c_0 \left(1 - r_1^{max} \frac{1}{r_0}\right)$$

Also $c_0 = c_0(g_1)$. Using the next lemma below and assuming $\psi > 1$, it can be shown, that $c_0(g_1) \geq c_0(g_0) \geq \frac{\psi - 1}{1 - \gamma} g_0 \equiv \underline{c}$. We conclude

$$\underline{C} \equiv \underline{c} \left(1 - r_1^{max}(g_1) \frac{1}{r_0}\right)$$

is a lower bound on $\underline{A}$. It is also a linear function in g_1 with a negative coefficient $-1/(r_0(\gamma - 1))$. Hence it is positive and unbounded as $g_1 \to -\infty$.

□

[3] We return to the continuity of the g_1 dependence below.

Lemma A.4. *Assume $\psi > 1$. For large S, the welfare benefit of ending a disaster, $V(g_1)$, is a continuous decreasing function and $V(g_0) = 0$.*

Proof. First we note that we are implicitly assuming the parameters are such that HJB system in Proposition 1 has a positive solution. The proof of that proposition required the conditions $g_1 \leq g_0$ and that g_1, g_0, and $\theta \equiv \frac{1-\gamma}{1-1/\psi}$ have the same sign. Here we are imposing $\psi > 1$ and earlier we took $\gamma > 1$. Hence, below we have that all three of these quantities are negative.

Define $\mathcal{R} = H(s=1)/H(s=0)$. Then $V = 1 - \mathcal{R}^{\frac{1}{1-\gamma}}$ is an increasing function of $\mathcal{R}$. We will establish that $\mathcal{R}$ is decreasing in g_1.

For $s \geq 1$, define $\tau = (S+1-s)/(\lambda S)$ and let $\mathcal{R}(\tau) = H(s+1)/H(s)$. For large S, the HJB system becomes the two-equations

$$g_0 = e_0 H^{e_1}(0) + \eta(\mathcal{R} - 1) \tag{A.51}$$

and

$$g_1 = e_0 H^{e_1}(\tau) - \frac{1}{H(\tau)} \frac{dH}{d\tau} \tag{A.52}$$

where $e_1 = -\psi\theta > 0, e_0 = \theta\rho^{\psi}/\psi < 0$. The latter ODE has solution that satisfies

$$H^{-e_1}(\tau) - \frac{e_0}{g_1} = \left[H^{-e_1}(0) - \frac{e_0}{g_1} \right] e^{g_1 e_1 \tau}.$$

Our definition of $\mathcal{R}$ equates to $H(1/\lambda)/H(0)$. Evaluating the expression above at $\tau = 1/\lambda$, multiplying by $H^{e_1}(0)$, using (A.51), and rearranging leads to the following algebraic equation for $\mathcal{R}$:

$$\mathcal{R}^{-e_1} + (1 - e^{g_1 e_1/\lambda}) \frac{\eta}{g_1} (\mathcal{R} - 1) - \left(e^{g_1 e_1/\lambda} + \frac{g_0}{g_1} (1 - e^{g_1 e_1/\lambda}) \right) = 0. \tag{A.53}$$

It can be immediately verified that $\mathcal{R} = 1$ at $g_1 = g_0$.

Since $e_1 > 0, g_1 < 0$, we have $e^{g_1 e_1/\lambda} < 1$. Then writing

$$\mathcal{R}^{-e_1} = -(1 - e^{g_1 e_1/\lambda}) \frac{\eta}{g_1} (\mathcal{R} - 1) + \left(e^{g_1 e_1/\lambda} + \frac{g_0}{g_1} (1 - e^{g_1 e_1/\lambda}) \right).$$

The left side is monotonically declining in $\mathcal{R} \geq 1$ from one to zero. The right side is an increasing linear function of $\mathcal{R}$. Its intercept is $e^{g_1 e_1/\lambda} + \frac{g_0}{g_1}(1 - e^{g_1 e_1/\lambda})$, and this is less than one because $g_1 < g_0$ and $\frac{g_0}{g_1}(1 - e^{g_1 e_1/\lambda}) < (1 - e^{g_1 e_1/\lambda})$. This guarantees a finite solution for $\mathcal{R}$ for any $g_1 < g_0$. Continuity in g_1 follows from existence of a solution and continuity of coefficients in g_1.[4]

Finally, implicitly differentiating with respect to g_1, it is straightforward to verify that the derivative is negative using $1 - e^{g_1 e_1/\lambda} < -g_1 e_1/\lambda$.

□

Proof of Proposition

Given the lemmas above, the bounds asserted in the proposition can be written

$$[\lambda V(\mathcal{R}(g_U)) \, , \, \lambda V(\mathcal{R}(g_L))]$$

where $1/\lambda = \mathbb{E}[T^\star]$ and $\mathcal{R}$ is defined in (A.53) and g_L, g_U are the solutions to (A.49)-(A.50).
QED

Timing Parameters

The figure below plots the numerically computed bounds identified in Proposition 4 using the baseline parameters from Table 1 in Section 2. The proof of the proposition relies on the large-S limit of the model. So the figure shows those limits relative to an equivalent small-S case to verify that the differences are negligible. The bounds could also depend on *when* during the disaster (measured by s/S) the stock market response to duration news is measured. The figure also shows that measuring the market response earlier (e.g., $s = 1$) is *conservative* in the sense that the implied welfare gains for a given market response increase with s.

[4]Continuity of $\mathcal{R}$ also implies continuity of the consumption function in g_1. This was used in the prior lemma.

Figure A.1: Welfare Gain Bounds as a Function of Timing parameters

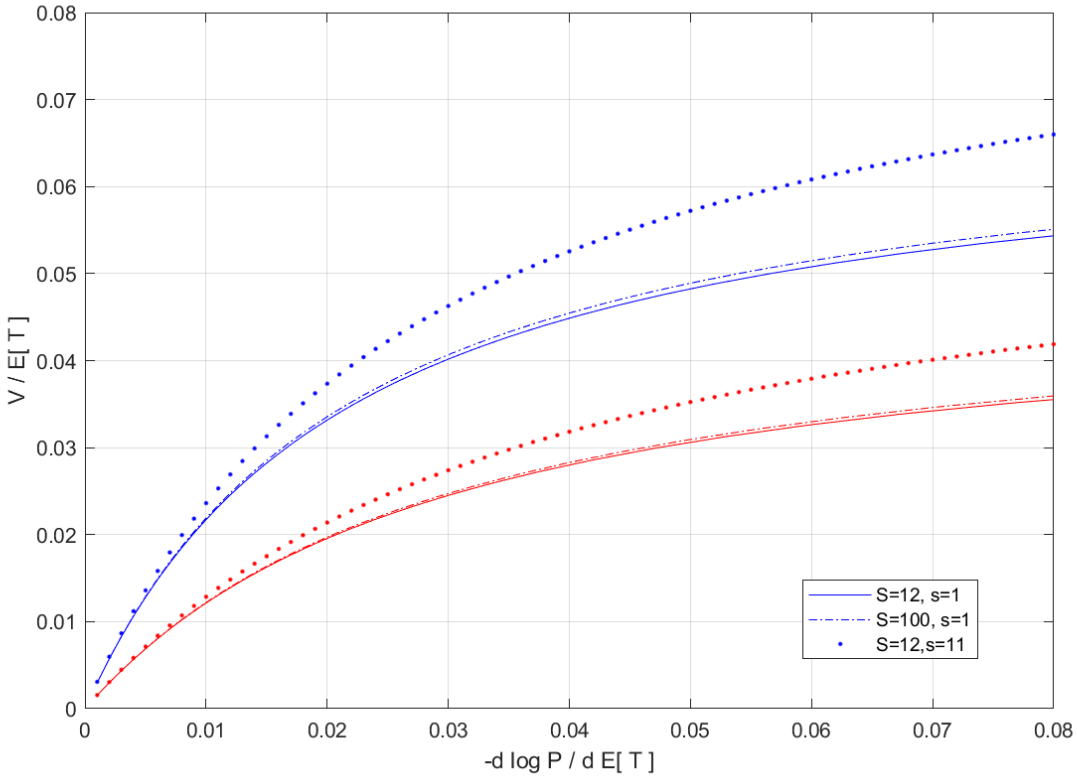

The Figure shows the minimum and maximum allowable welfare gain to ending a disaster given an observed stock market response to disaster duration news. The bounds are shown for three choices of the timing parameters, as shown in the legend.

A.5 Output Claim

The model in Section 2 views the stock market as a claim to the economy's future output flow, defined as the change in the stock of wealth before consumption. This subsection clarifies the reasons for this definition, offers a decentralization that supports it, and also notes alternative claims that can achieve the same objectives.

First, our aim is to tractably depict a market that responds to news about disaster duration, as captured by the state variable s. As is well known, in an economy where the

capital stock can be costlessly converted to consumption goods, the unit price of the capital stock is constant and equal to 1.0. Or, in our notation, the value of q is q. Moreover, this is also equal to the value of a claim to all future consumption. In many applications, this is a reasonable depiction of the market portfolio. But it does not describe the dynamic that we are interested in modeling.[5] As noted in the text, it is standard in the macro-finance literature to assume a process for dividends that is more volatile and more procyclical than consumption in order to match asset pricing moments. Similarly, in our case, we need a dividend process that is more "procyclical" in its exposure to disaster risk. The output claim achieves this because its expected cash flow mirrors the impact on wealth of the pandemic.

To see how the flow that we are valuing could constitute the payouts to owners of corporate claims, consider the following decentralization.

1. Households own the capital stock and rent it to goods-producing firms.
2. Firms produce output $\mu(s)\ q\ dt + \sigma(s)\ q\ dW_t$ per unit time.
3. Firms purchase insurance against pandemic shocks $-\chi\, q\, dJ$ from an insurance sector.
4. The market portfolio consists of a claim to the profits of both sectors plus the rental contract for the capital stock.

Notice that in step 1, the rental is effectively a riskless bond in that the "face value" of q is insured. Thus, in this economy households separate risky and safe claims.

Having equity holders effectively bear the risk of disaster shocks can be similarly achieved by envisioning a labor contract that insures workers. Suppose aggregate wages are $W = \phi C + (1-\phi) i(s)$ where C is aggregate consumption and $i(s)$ is the expected disaster loss rate $\chi\zeta\ q$ when $s > 0$. Then we can let equity represent a claim to the dividend stream $(C - W)dt$. Figure A.2 shows the disaster sensitivity of this claim using our baseline parameters. Since it behaves similarly to the output claim, the paper's results are robust to using this alternative claim.

[5] Recall that in our model changes in the state s do not directly alter q.

Figure A.2: Disaster Sensitivity of Assets

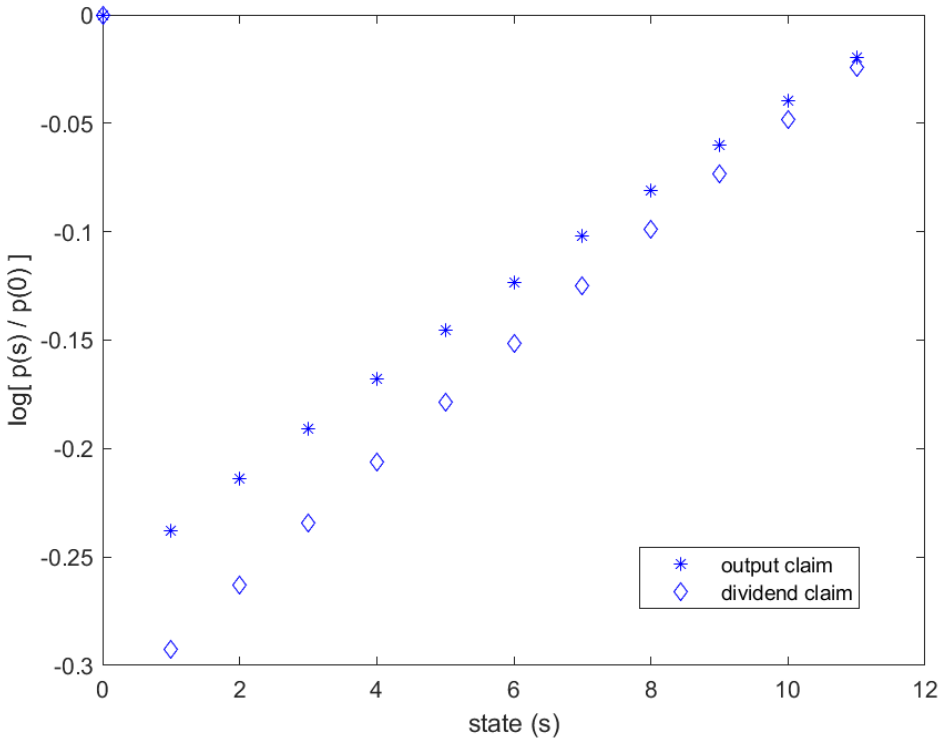

The Figure shows the log of the price-capital ratio in disaster states relative to its value in the non-disaster state for the claim to output and the claim to dividends, as described above. The parameters are those used in Section 4 of the text.

B Vaccine Progress Indicator

This section includes additional details on construction of the vaccine progress indicator. Each day's forecast is computed via simulation as described in Section 3 of the paper. The procedure is depicted graphically in the flow chart Figure A.3.

The simulation takes as input a timeline of COVID-19 vaccine candidates' stage-by-stage progress from the London School of Hygiene & Tropical Medicine.[6] We observe the start dates of each pre-clinical and clinical trial, along with their vaccine strategy. Table A.1 breaks down the number of candidates at each state at the end of our sample. Table

[6]We use the timeline available on November 2, 2020.

Figure A.3: Simulation Flow Chart

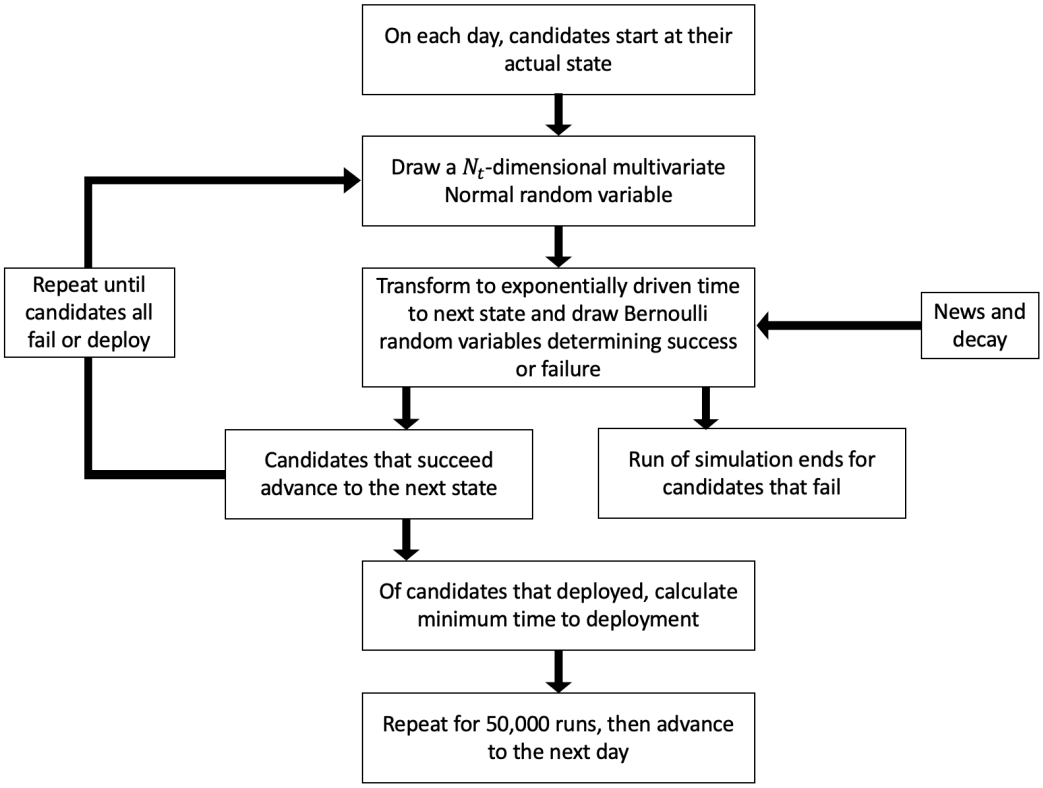

Note: Figure shows the simulation that estimates the expected time until vaccine deployment.

A.2 summarizes the main strategies along with the number of candidates following each.

We collect all clinical-trial news articles from FactSet StreetAccount during our sample period. Table A.3 shows the number of articles by news type, while Table A.4 shows the top ten candidates by news count.

Each candidate may simultaneously be run in seveal clinical trial sequences (e.g., with different patient populations or delivery modalities). Following Wong et al. (2018), we adopt each candidate's most advanced branch. Since candidates share a common virus target, and potentially common institutes or strategies, we define pairwise correlations in

Table A.1: Vaccine States

State	# Candidates	Example Candidates
Preclinical	210	Amyris Inc Baylor College of Medicine Mount Sinai
Phase I Safety Trials	20	Clover/GSK/Dynavax CSL/University of Queensland Imperial College London
Phase II Expanded Trials	18	Arcturus/Duke Osaka/AnGes/Takara Bio Sanofi Pasteur/GSK
Phase III Efficacy Trials	11	AstraZeneca/Oxford BioNTech/Fosun/Pfizer Moderna

Note: Table describes the number of vaccine candidates in each state, along with example institutes. Data are from the London School of Hygiene & Tropical Medicine's COVID-19 Tracker. Data are as of November 2, 2020.

an additive manner. For two candidates $n \neq n'$:

$$\rho(n,n') = \begin{cases} 0.2 & \text{baseline} \\ \text{add } 0.2 & \text{if shared institute} \\ \text{add } 0.1 & \text{if shared strategy.} \end{cases}$$

Table A.5 lists our parameter choices of durations and baseline probabilities of success. Our baseline success probabilities are based upon estimates in Pronker et al. (2013), and augmented by our own sample of historical outcomes of infectious disease vaccine trials from pharmaceutical research firm BioMedTracker. Our baseline duration estimates are based on projections from the pharmaceutical and financial press during 2020.

Table A.6 summarizes the distribution of time spent in each state in our simulation. We track days spent in each state until the next state starts, only among candidates that have successfully transitioned to the next state. The realized outcomes for durations are

Table A.2: Vaccine Strategies

Type	Description	# Candidates
RNA (genetic)	Consist of messenger RNA molecules which code for parts of the target pathogen that are recognised by our immune system ('antigens'). Inside our body's cells, the RNA molecules are converted into antigens, which are then detected by our immune cells.	33
DNA (genetic)	Consist of DNA molecules which are converted into antigens by our body's cells (via RNA as an intermediate step). As with RNA vaccines, the antigens are subsequently detected by our immune cells.	21
Viral Vector	Consist of harmless viruses that have been modified to contain antigens from the target pathogen. The modified viruses act as delivery systems that display antigens to our immune cells. Replicating make extra copies of themselves in our body's cells. Non-replicating do not.	56
Protein	Consist of key antigens from the target pathogen that are recognised by our immune system.	78
Inactivated	Consist of inactivated versions of the target pathogen. These are detected by our immune cells but cannot cause illness.	16
Attenuated	Consist of living but non-virulent versions of the target pathogen. These are still capable of infecting our body's cells and inducing an immune response, but have been modified to reduce the risk of severe illness.	4

Note: Table describes the number of vaccine candidates in each strategy. 51 candidates have other, virus-like particle or unknown strategies. Data from the London School of Hygiene & Tropical Medicine's COVID-19 Tracker. Data as of November 2, 2020.

reasonably consistent with our choices of parameters, in particular for Phase I and Phase II. The fact that the standard deviations of durations are less than the mean is consistent with the Gaussian copula assumption of positively correlated outcomes.

We then augment π_s^{base} with 233 news articles from FactSet StreetAccount, split into positive and negative news types. Table A.7 lists the news types along with their changes in probabilities.

Table A.3: Number of Articles by News Type

News Type	Number of Articles
Release positive data	79
Announce next state	45
Positive regulatory action	30
Positive preclinical progress	22
Announce dosage start	21
Positive enrollment	17
State ahead of schedule	7
State resumed	5
State paused	4
State behind schedule	1
Negative regulatory action	1
Negative enrollment	1
Total	233

Note: Table shows the count of news articles by news type.

Table A.4: Number of Articles by Top 10 Candidates

Candidate	Number of Articles
Moderna	37
BioNTech / Fosun Pharma / Pfizer	25
Oxford / AstraZeneca	23
Johnson & Johnson / Beth Israel Deaconess Medical Center	21
Inovio Pharmaceuticals	18
Novavax	14
Arcturus / Duke	10
Vaxart	9
Medicago / GSK / Dynavax	8
Takis / Applied DNA / Evvivax	8

Note: Table the number of news articles for the top ten candidates by article count.

Table A.5: State Durations and Probabilities of Success

State	τ_s (years)	π_s^{base} (%)
Preclinical	0.6	5
Phase I	0.2	70
Phase II	0.2	44
Phase III	0.4	69
Application	0.1	88
Approval	0.5	95

Table A.6: Vaccine States

	Days in State				
	Min	Max	Mean	Median	SD
Preclinical	1.0	233.0	94.6	90.5	59.2
Phase I	17.0	103.0	51.9	27.0	39.8
Phase II	6.0	152.0	86.8	89.0	54.5

Note: Table shows statistics on days spent in each state before transitioning, among candidates that have successfully transitioned to the next state. Data are from the LSHTM and are as of November 2, 2020.

Table A.7: News and Changes in Probabilities

Positive		Negative	
News type	$\Delta\pi$ (%)	News type	$\Delta\pi$ (%)
Announce next state	+5	Pause in state	-25
State ahead of schedule	+2	State behind schedule	-15
Release positive data	+5	Release negative data	-60
Positive regulatory action	+3	Negative regulatory action	-50
Positive preclinical progress	+1	Negative preclinical progress	-2
Positive enrollment	+1	Negative enrollment	-5
Dose starts	+1		
State resumes after pause	+5		

Note: Table shows the positive and negative news types, along with their changes in probabilities.

C Extensions

This appendix considers some generalizations of the model. We demonstrate that these extensions are unlikely to alter the primary conclusions of the paper concerning the ex ante welfare benefit of curtailing the COVID-19 pandemic.

C.1 Endogenous Vaccine Development

The model in Section 2 includes no actual vaccine development (or disaster mitigation) technology. The reason for this is simply that parameterizing and calibrating a biopharmaceutical R&D production function is beyond the scope of the study. However, there could be a concern that we overstate the value of ending the pandemic by not giving the economy a real option to address it. We now show a tractable way to do this, and we explain why our results are consistent with this extension. In a nutshell, optimal research effort will impose a constraint on the parameters that does not affect our empirical identification of the pandemic duration and severity.

Suppose that, when a pandemic arrives, the representative agent has the ability to choose an expenditure rate ι that increases the arrival rate of vaccine progress. The most parsimonious specification would just be linear:

$$\lambda(\iota) = L_0 + L_1\,\iota.$$

(The discussion will treat the 2-state model. Generalization to S-states is straightforward.) Given the rate, the dynamics of wealth, dq/q, picks up a new term $-\iota\,dt$ for the duration of the pandemic. Without loss of generality, we can assert that whatever ι level the agent chooses in the first pandemic is also optimal for all subsequent pandemics. For notational simplicity below, define the adjusted drift during the pandemic as

$$\mu_S(\iota) = \mu(1) - \iota$$

where $\mu(1)$ is the benchmark growth rate without research effort. While this formulation is too sparse to address issues of public versus private returns to research expenditure, it does allow us to formulate and solve a model in which vaccine progress (and exiting from pandemic) is an endogenous outcome.

Notice that, given a choice of ι, the economy behaves exactly as in our reduced-form case. Hence the solution for optimal consumption and the value function are unchanged. In particular, we can write the value function within the pandemic as $H(1;\lambda(\iota),\mu_S(\iota))$. To choose the optimal policy, ι^*, the agent simply maximizes this function. This verifies that the optimal rate is constant within a state and does not vary across pandemics. Of course, a necessary condition for an interior optimum is

$$\frac{\partial H}{\partial \mu_S} = L_1 \frac{\partial H}{\partial \lambda}.$$

Optimality of the research effort does constrain admissible pairs of λ and μ_S via this relation.

Clearly in an economy with powerful research technology (where L_1 is a large number), agents can make the pandemic very brief (in expectation) at low cost. Hence, the endogenous value of λ would be high, and agents would pay less to return to the non-pandemic state than in an economy with inferior vaccine technology. However, recall that our benchmark calibration above already conditioned on different values of λ. We showed that the welfare gain depended strongly on the remaining expected duration of the pandemic, which could be inferred in the data from our estimation of the expected time to deployment of a vaccine during 2020.

Now, taking λ as fixed at an observed value $\hat{\lambda}$ say, consider the ratio

$$f(\hat{\mu}_S) = \left.\frac{\partial H}{\partial \mu_S}\right|_{\hat{\lambda},\hat{\mu}_S} \Big/ \left.\frac{\partial H}{\partial \lambda}\right|_{\hat{\lambda},\hat{\mu}_S}.$$

Given any value of the technology parameter L_1, the first order condition above requires us to use the value of $\hat{\mu}_S$ satisfying $f(\hat{\mu}_S) = L_1$. Assuming a solution exists, this is the full economic content of endogenizing vaccine investment in this setting.

Would imposing such a restriction on μ_S affect our estimated welfare results? To see why it will not, recall from Section 2.6 that the stock market response to news about the state (i.e., vaccine progress) effectively identifies the welfare gradient directly. The precise choice of individual model parameters is, to a first approximation, irrelevent, conditional on matching this moment. Requiring that μ_S satisfies the above first order condition would take away one degree of freedom in the calibration. But choosing the remaining

disaster parameters (e.g. χ) to yield the same stock market response would restore the same empirical conclusions.

To be clear, the conclusion is not that including a vaccine development technology does not affect the welfare costs of the pandemic. Rather, we are pointing out that our empirical work has already pinned down the key inputs to that value. Taking those quantities at face value, adding assumptions about the development technology and imposing the restriction of optimal investment do not perturb the calculation.

C.2 Endogenous Pandemic Severity via Labor Choice

Another concern with our reduced-form model is that it omits mechanisms by which agents' choices may affect the severity of the disaster. In this appendix, we develop a version of the model in which the household (or a social planner) trades off economic growth for exposure to the disaster. Again with COVID-19 in mind, the trade-off is between supplying labor (and increasing the individual's risk of infection) and lock-down.

In this version of the model, wealth accumulates according the stochastic process

$$dq = \ell^{\alpha} q\mu dt - Cdt + \sigma \ell^{\alpha/2} q dB_t \tag{A.54}$$

in the non-pandemic state, and

$$dq = \ell^{\alpha} q\mu dt - Cdt + \sigma \ell^{\alpha/2} q dB_t - [\ell\varepsilon + k + KL] q dJ_t. \tag{A.55}$$

in the pandemic state. As before, C is the endogenous consumption rate, and now ℓ is the household's labor supply, and $\alpha \in (0,1)$ is the elasticity of expected output with respect to labor. The results below all go through with constant returns to scale in the drift term. Both individual and aggregate labor are assumed to affect the agent's exposure to the health shock via the jump size. Let

$$\chi(\ell, L) \equiv [\ell\varepsilon + k + KL], \tag{A.56}$$

where ε is exposure to the pandemic via private labor, k is exposure to the pandemic unrelated to labor, L is aggregate labor supply, and K is exposure via aggregate labor. These parameters can capture losses of wealth due to health-induced disruptions to work, the

need to work from home with attendant productivity impact and loss of human capital, deadweight losses from bankruptcy, and frictions from labor reallocation. We will assume parametric restrictions on ε, k and K to be such that $(1-\chi) \in (0,1)$. The agent takes the aggregate supply of labor L as given in her optimization problem.

Agents' preferences are as in the text. We assume no disutility to labor supply and no frictions in adjusting ℓ. We assume $\ell \in [0, \overline{\ell}]$, where the upper bound $\overline{\ell}$ is the agents' total available work capacity.

The agent's problem is now to choose in each state s optimal consumption $C(s, L^*(s))$ and labor $\ell(s, L^*(s))$ that maximizes the objective function. We impose that agents have rational expectations about $L^*(s)$, the aggregate labor in equilibrium. In other words, individual agents' decisions in the aggregate imply a wealth (consumption) dynamic that is confirmed in equilibrium. Hence, the wealth dynamic in the pandemic regime must be:

$$dq(s) = [\ell(s, L^*(s))]^{\alpha} q\mu dt - C(s, L^*(s))dt + \sigma[\ell(s, L^*(s))]^{\alpha/2} q dB - \chi(\ell(s, L^*(s)), L^*(s)) q dJ_t \tag{A.57}$$

Since $L^*(s)$ is a constant for each s, the above dynamics are identical to those assumed by the agent. Substituting for the equilibrium fixed point that $L^*(s) = \ell(s, L^*(s))$, we can then obtain the equilibrium outcomes.

Proposition 1. *Equilibrium labor in the non-pandemic state is given by*

$$L(0) = L(S) = \overline{\ell} \tag{A.58}$$

Equilibrium labor in pandemic states $L^*(s)$ $\forall s \in \{1, \ldots, S-1\}$ solves[7]

$$\chi(L(s), L(s)) = k + (\varepsilon + K)L(s) = \left[1 - (L(s))^{\frac{1-\alpha}{\gamma}} \nu\right] \tag{A.59}$$

where

$$\nu \equiv \left[\frac{\alpha\left(\mu - \frac{1}{2}\gamma\sigma^2\right)}{\zeta\varepsilon}\right]^{-\frac{1}{\gamma}}. \tag{A.60}$$

[7] It can be shown that given $\alpha \in (0,1)$, the second order condition for a maximum is satisfied whenever $\mu - \frac{1}{2}\gamma\sigma^2 > 0$, which also implies $\nu > 0$.

Proof. The HJB equation for each state $s \in \{1,\ldots,S-1\}$ is now

$$0 = \max_{C,\ell} \Big[f(C,\mathbb{J}(s,q)) - \rho\mathbb{J}(s,q) + \mathbb{J}_q(s,q)(\ell^\alpha q\mu - C) + \frac{1}{2}\mathbb{J}_{qq}(s,q)\ell^\alpha q^2\sigma^2 + \zeta\left[\mathbb{J}(s,q(1-\chi)) - \mathbb{J}(s,q)\right] + \lambda_u(s)\left[\mathbb{J}(s+1,q) - \mathbb{J}(s,q)\right] + \lambda_d(s)\left[\mathbb{J}(s-1,q) - \mathbb{J}(s,q)\right]\Big] \tag{A.61}$$

Using the conjecture for the objective function in the text for $\mathbb{J}(s)$, calculating the derivatives with respect to q, $\mathbb{J}_q = H(s)q^{-\gamma}$ and $\mathbb{J}_{qq} = -\gamma H(s)q^{-\gamma-1}$, and differentiating with respect to labor ℓ, we obtain the first-order condition as

$$\mathbb{J}_q(q)\alpha\ell^{\alpha-1}\mu q + \frac{1}{2}\mathbb{J}_{qq}(q)\alpha\ell^{\alpha-1}\sigma^2q^2 - \mathbb{J}_q\left(q(1-\chi)\right)\zeta\varepsilon q = 0 \tag{A.62}$$

where we have suppressed state s in the notation. This in turn simplifies to

$$\left[\frac{\alpha\left(\mu - \frac{1}{2}\gamma\sigma^2\right)}{\zeta\varepsilon}\right]\ell^{\alpha-1} - [1-\chi]^{-\gamma} = 0 \tag{A.63}$$

where $\chi(\ell,L) = k + \varepsilon\ell + KL$. In rational expectations equilibrium $L(s) = \ell(s)$, which gives us that optimal labor in pandemic state $L^\star(s)$ $\forall s \in \{1,\ldots,S-1\}$ satisfies (A.59):

$$\chi\left(L(s),L(s)\right) = k + (\varepsilon+K)L(s) = \left[1 - (L(s))^{\frac{1-\alpha}{\gamma}}\nu\right] \tag{A.64}$$

where

$$\nu \equiv \left[\frac{\alpha\left(\mu - \frac{1}{2}\gamma\sigma^2\right)}{\zeta\varepsilon}\right]^{-1/\gamma}. \tag{A.65}$$

For the non-pandemic state $s = 0$ or $s = S$, the third term in first-order condition (A.62) is absent; therefore, we obtain that labor is at the highest possible level $L(0) = L(S) = \overline{\ell}$, whenever $\alpha\left(\mu - \frac{1}{2}\gamma\sigma^2\right) > 0$. □

In the non-pandemic state, the agent faces no cost to supplying labor and exerts effort fully. However, in the pandemic states, the agent increases exposure to health risk by supplying labor, which creates a tradeoff between augmenting the capital stock and

reducing the loss of human capital that arises from health shocks.[8]

Given the optimal labor and consumption policies, the model solutions in Section 2 can be directly applied. As before, the pandemic parameters only enter the system of equations via the constants g_0 and g_1, which we can write compactly as

$$g(x,y) \equiv \frac{(1-\gamma)\rho}{(1-\psi^{-1})} - x^{\alpha}(1-\gamma)\left(\mu - \frac{1}{2}\gamma\sigma^2\right) - y\left(\left[1-\chi(x,x)\right]^{1-\gamma} - 1\right) \tag{A.68}$$

with $g_0 = g(\overline{\ell},0)$ and $g_1 = g(\ell(s),\zeta)$.

As in the previous section, estimating the key parameters in this extension of the model – those determining the elasticity of health risk to labor supply and the degree of the health externality – is beyond the scope of the paper. However, again, we can affirmatively demonstrate that the endogenous determination of the pandemic severity has no effect on our primary finding that the stock market reaction to pandemic duration news effectively identifies the welfare benefit of ending the pandemic. Figure A.4 reproduces the computation of Figure 4 using the baseline parameters from Table 1 in the text and varying the new parameters k, K, and ε over wide ranges, given in the figure caption.[9] The figure verifies that differing parameter values lead to different endogenous levels of disaster severity, as measured by the welfare cost. However, just as in Section 4, the computation affirms that this variation in welfare costs also leads to variation in the stock market response to pandemic news, and that the latter pins down the former.

[8]Note the externality in our set up via the KL term in the size of the helath shock that is not internalized by each agent. A central planner would factor this in the socially efficient choice of labor. This is tantamount to replacing ε by $(\varepsilon + K)$ in ν above to obtain ν^{CP}:

$$\nu^{CP} \equiv \left[\frac{\alpha\left(\mu - \frac{1}{2}\gamma\sigma^2\right)}{\zeta(\varepsilon+K)}\right]^{-\frac{1}{\gamma}} \tag{A.66}$$

Socially efficient labor choice $L^{CP}(s)$ in the pandemic states is then given by

$$\chi(L(s),L(s)) = k + (\varepsilon+K)L(s) = \left[1 - (L(s))^{\frac{1-\alpha}{\gamma}}\nu^{CP}\right] \tag{A.67}$$

It is then straightforward to show that $\nu^{CP} > \nu$ for $K > 0$ and $\gamma > 0$, and hence $L^{CP}(s) < L(s)$, i.e., the socially efficient choice of labor in pandemic states is smaller than the privately optimal one.

[9]The exercise fixes the labor-share parameter to be $\alpha = 0.7$ and the intensity of the health shocks to be $\zeta = 1$. Including variation in these values does not affect the level or range of the curve plotted in the figure.

Figure A.4: Stock Market Sensitivity and Welfare Loss Rate

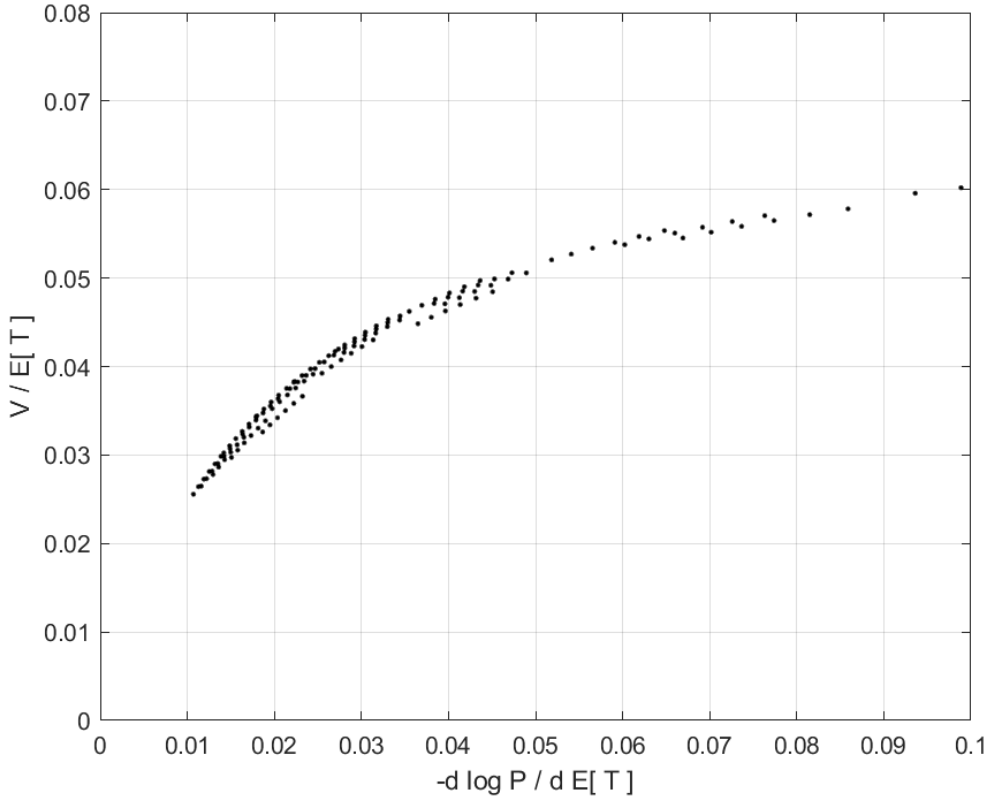

The Figure shows the welfare cost per unit (expected) time, $V/\mathbb{E}[T^\star]$ as a function of the stock market sensitivity to changes in the expected time $-\Delta \log P/\Delta \mathbb{E}[T^\star]$ as the current state s increases by 1. Each point corresponds to a different set of labor parameters. The ranges of these parameters are $k \in [0.001, 0.006], K \in [0.02, 0.10], \varepsilon \in [0.012, 0.024]$. We fix $\alpha = 0.7$ and $\zeta = 1$. The remaining parameters are those given in Table 1.

C.3 Limited Participation

Our analysis has been conducted from the point of view of a representative household/investor who both experiences the negative shocks of the pandemic and prices financial claims. It is reasonable to ask how our results should be interpreted in a world where a large segment of the population does not participate in asset markets. What, if anything, can we say about the ex ante welfare cost of the pandemic for nonparticipants? The answer depends upon the similarity of the pandemic experience for nonparticipants and partici-

pants, and also upon the interaction between the two groups.

Under autarky, where nonparticipants do not affect financial markets at all, we can still view them as having a value of human capital $\tilde{q}$ equal to the present value of their lifetime consumption. If we assume that shocks to $d\tilde{q}$ are affected by the pandemic in a stochastically similar manner to what we have estimated for participants (i.e. to dq), then the welfare cost, or welfare benefit of ending the pandemic for nonparticipants can be estimated from our results, conditional on their preferences. Several important studies in the literature on nonparticipation, including Gomes and Michaelides (2008) and Guvenen (2009), suggest that nonparticipants have a significantly lower elasticity of intertemporal substitution than participants. Both studies employ a value of 0.1. Using our baseline parameter estimates under which the welfare cost at the beginning of the pandemic is 4.80% percent of wealth per year of expected duration for participants with an EIS of 1.5, the cost to an agent with an EIS of $\psi = 0.1$ is 4.72%. There is less consensus on nonparticipants' rate of time preferences, but it is reasonable to suppose that they may be more impatient than participants. Redoing the welfare calculation for an agent with $\rho = 0.04$ and $\psi = 0.1$ yields a welfare cost of 4.70% of her wealth per year.[10] In other words, the paper's primary finding on the welfare cost of the pandemic - or the willingness to pay to curtail it – apply very closely to nonparticipants as well as participants.

Of course, this conclusion may not go through if the two groups face different exposure to the pandemic. On the one hand, nonparticipants may face more danger to their (human) wealth due to worse access to healthcare or less ability to work at home, for example. In this case, the willingness of nonparticipants to pay to end the pandemic would be higher than those that we have estimated.

On the other hand, in models such as Danthine and Donaldson (2002) and Guvenen (2009) participants provide a degree of insurance to nonparticipants (via wage contracts or the bond market or government transfers). In this class of models, the two groups do interact nontrivially, and financial market properties depend on the details of the contracting. However, if the net result is that participants shield nonparticipants from some of the dangers of the pandemic, the latter group would have a lower willingness to pay to end the pandemic.

[10] Since it is generally not possible to empirically identify nonparticipants' risk aversion in the data, the calculation assumes $\gamma = 4$, as in the baseline case.

D Interpreting the COVID-19 stock market experience

For tractability, our model omits many factors that played important roles in 2020. We have not included fiscal or monetary policy, for example. (Recall, though, that our empirical work excluded large market-moving events attributable to non-vaccine news as classified in Baker et al. (2020)). We now describe in more detail its implications for the response of the stock market and of consumption to a pandemic. Comparing these implications to the actual experience of 2020, we argue that a coherent interpretation is possible when viewed through the lens of the model. Hence, while there are inevitably descriptive limitations, these need not detract from the paper's objectives.

Consider first the **stock market**. From December 31, 2019 to March 23, 2020 the CRSP value-weighted experienced a return of approximately -36%, continuously compounded. The market then rebounded fully by early autumn. The cumulative return for the year was approximately +5% at end of October (where our clinical trial sample stops).

The calibration in the paper implies a somewhat smaller drop, of -25% for the output claim at the onset of a pandemic, based on our initial VPI forecast of an expected duration of four years. Thus, relative to this data point, our estimation of the potential damage of the pandemic is conservative compared to the market's assessment.

Subsequently, the model implies a partial market recovery due to the observed success of vaccine trials. From March 23 through October 30, our forecast of the pandemic's duration dropped by 2.5 years, of which 0.6 years was expected. The implied market response to this progress – calibrated to match the response estimated in our empirical work – is approximately 16%.

Thus, without conditioning on any other shocks, the basic dynamics of our model can account for approximately 70% of the observed market decline and about one-third of the recovery through our sample period. To shed light on factors the model may be missing, it is useful to decompose the initial market decline into components due to cash flow news, real interest rate news, changes in the equity risk premium. One way to identify these return components, r^{CF}, r^{RF},and r^{RP} within the model is as follows.

1. Assume that, on a switch to a pandemic, the parameters of the process dq change as described in Section 2. Solve the asset pricing system given in Proposition 3, but without any risk-adjustments (i.e., under the physical measure) and fixing the

riskless rate in the pandemic, $r(1)$, to be its non-pandemic value, $r(0)$, as computed under the original benchmark calibration.

- Call the resulting price-dividend ratio $\tilde{p}(s)$.
- Define the percent change in this on entering the pandemic $r^{CF} = \log(\tilde{p}(1)/\tilde{p}(0))$ to be the return due to cash flow news.

2. Solve the same pricing system, still under the physical measure, but now allowing $r(1)$ to be its pandemic value in the calibrated model.

   - Call the new price-dividend ratio $\hat{p}$.
   - Call $r^{RF} = \log(\hat{p}(1)/\hat{p}(0)) - r^{CF}$ the return due to real interest rate news.

3. As in the text, let $p(s)$ denote the price-dividend ratio under the full model.

   - Call the residual $r^{RP} = \log(p(1)/p(0)) - r^{RF} - r^{CF}$ the return due to risk premium news.

With the baseline calibration the results are:

$$r^{CF} = -0.328, \qquad r^{RF} = 0.284, \qquad r^{RP} = -0.206.$$

Recently, Knox and Vissing-Jorgensen (2022) report empirical estimates of the same decomposition during 2020 using information in options markets, inflation swaps, and S&P 500 dividend futures. Consistent with their work, we find substantial and nearly offsetting positive and negative components of discount rate news, that is $r^{RF} + r^{RP}$ is small.

The risk premium component in our model is due to the threat of Poisson shocks. As is well-known from the long-run risk literature, investors with Epstein-Zin preferences and $\gamma > 1/\psi$ are averse to uncertainty and growth-rate risk. Also, in the model, real rates decline on entering the pandemic with the riskless rate turning mildly negative, consistent with the data.

Our model attributes large effects to cash flow news. In fact, expected cash flows did decline steeply in early 2020: December 2020 S&P 500 dividend futures declined

more in percentage terms than did the overall stock market,[11] However, as Knox and Vissing-Jorgensen (2022) show, near-term dividends makes up a small component of market value. So declines in the discounted sum (e.g., for 10 years ahead) cannot account for a large component of the market drop. As a result, and combined with the small net discount rate effects, the authors attributing most of the market decline to residual unidentified long-term effects.

In our model, there are both short-term cash-flow effects from lower output, as well long-term effects from the loss of part of the capital stock. Evidently the market was anticipating less short-run impact, but greater long-term impact, perhaps due to scarring type effects that are absent from the model. Recall that, while we assume permanent effects of the pandemic on the level, q, we assume purely transitory effects on the growth rate of dq once the pandemic ends. The market may have not been so sure.

Turning to the implication for our conclusions, it is clear that adding negative long run effects in order to match the observed market decline (while holding other return components fixed) will imply larger welfare gains to mitigating the pandemic. It is important to recognize that, while the model's return decomposition can be altered (e.g., with different preference parameters), this will not necessarily lead to large welfare effects if we still impose that the calibration matches the magnitude of the market response to vaccine progress. As described in the text, the latter condition effectively pins down the severity of the pandemic.

Next consider the path of **consumption**. An extremely prominent feature of the 2020 experience was the rapid plunge in consumption in March and April followed by a complete rebound by early 2021. In the context of the model, consumption is driven primarily by the wealth process, dq. (The effect of changes in the marginal propensity to consume is second order.) A large decline in observed consumption is consistent with the occurrence of one or more down jumps in q in the early part of the year. These Poisson events are the way in which the pandemic is realized within the model. In fact, the early occurrence of such a shock – which was not considered above – can also bring the model's implied stock market decline directly into line with the observed fall.

[11] The December contract, quoted in units of the S&P 500 index, dropped from 62.5 at the end of 2019 to 39 on 3/23/20, a decline of 47%. Using this contract as a denominator, the price-dividend ratio on the market actually went up over this period.

However, as just discussed, the model has no mechanism for the reversal of these shocks after the pandemic ends, still less while the pandemic remains in progress. How, then, can the model explain the consumption rebound?

In our view, the most coherent interpretation of the consumption experience is that a large component of the recovery must be regarded as having been unexpected. Indeed, from the analysis above, it would be seemingly impossible to build a model in which a strong rebound in consumption is expected *ex ante* within a pandemic and in which the stock market drops nearly 40% due to the arrival of the pandemic. Moreover, the strong rebound in stock prices after March is also consistent with the interpretation of substantial unexpected good news about fundamentals, further helping to reconcile the model's implications of a rally only partially explained by vaccine progress. Moreover, evidence in Hong et al. (2021) and Gormsen and Koijen (2020), respectively, supports strong positive revision in corporate cash flows during the pandemic, by examining expectations of stocks' earnings and implied dividend yields.

In the context of the model, unexpected consumption changes are described by the Gaussian component of wealth shocks, which can be viewed as encompassing mechanisms like (unanticipated) policy interventions that are outside the model. Invoking large positive shocks is not implausible if the scale of these shocks, governed by $\sigma(s), s > 1$, is large. Our calibration uses $\sigma(s) = 0.075$ (or 3.75% per quarter) for the pandemic states. With this value, the 8% increase in consumption in the third quarter of 2020 is approximately a two standard deviation event (depending on the assumed conditional mean), unlikely but not impossible.

To summarize, fully accounting for the behavior of the financial markets and the real economy during 2020 is beyond the scope of our baseline stylized model. Nor is it the main objective of the paper. Nevertheless, the primary contours of the data can be reasonably described as an outcome within the model, given certain realizations of the stochastic shocks, as described above.

References

Scott R Baker, Nicholas Bloom, Steven J Davis, Kyle Kost, Marco Sammon, and Tasaneeya Viratyosin. The Unprecedented Stock Market Reaction to COVID-19. *The Review of Asset Pricing Studies*, 07 2020.

Jean-Pierre Danthine and John B Donaldson. Labour relations and asset returns. *The Review of Economic Studies*, 69(1):41–64, 2002.

Francisco Gomes and Alexander Michaelides. Asset pricing with limited risk sharing and heterogeneous agents. *The Review of Financial Studies*, 21(1):415–448, 2008.

Niels Joachim Gormsen and Ralph S J Koijen. Coronavirus: Impact on Stock Prices and Growth Expectations. *The Review of Asset Pricing Studies*, 10(4):574–597, 09 2020.

Fatih Guvenen. A parsimonious macroeconomic model for asset pricing. *Econometrica*, 77(6):1711–1750, 2009.

Harrison Hong, Jeffrey Kubik, Neng Wang, Xiao Xu, and Jinqiang Yang. Reopening effect of COVID-19 vaccines on corporate earnings. Technical report, Working Paper, October 2021.

Benjamin Knox and Annette Vissing-Jorgensen. A stock return decomposition using observables. Working paper, FEDS Working Paper, March 2022.

Esther S Pronker, Tamar C Weenen, Harry Commandeur, Eric HJHM Claassen, and Albertus DME Osterhaus. Risk in vaccine research and development quantified. *PloS one*, 8(3):e57755, 2013.

Chi Heem Wong, Kien Wei Siah, and Andrew W Lo. Estimation of clinical trial success rates and related parameters. *Biostatistics*, 20(2):273–286, 01 2018.